Journal of Power Sources 216 (2012) 323–329

Contents lists available at SciVerse ScienceDirect

Journal of Power Sources

journal homepage: www.elsevier.com/locate/jpowsour

Low-viscosity ether-functionalized pyrazolium ionic liquids as new electrolytes for lithium battery

Ming Chai [a], Yide Jin [a], Shaohua Fang [a,*], Li Yang [a,*], Shin-ichi Hirano [b], Kazuhiro Tachibana [c]

[a] School of Chemistry and Chemical Technology, Shanghai Jiaotong University, Shanghai 200240, China
[b] Hirano Institute for Materials Innovation, Shanghai Jiaotong University, Shanghai 200240, China
[c] Department of Chemistry and Chemical Engineering, Faculty of Engineering, Yamagata University, Yamagata 992-8510, Japan

HIGHLIGHTS

- New ether-functionalized pyrazolium ILs are reported.
- They have low-viscosity and low-melting point characteristics.
- Li/$LiFePO_4$ cells using these IL electrolytes have good electrochemical performance.

ARTICLE INFO

Article history:
Received 8 March 2012
Received in revised form
2 May 2012
Accepted 28 May 2012
Available online 1 June 2012

Keywords:
Ionic liquid
Lithium battery
Functionalized cation
Electrolyte

ABSTRACT

Four new functionalized ILs based on pyrazolium cations and bis(trifluoromethylsulfonyl)imide anions ($TFSI^-$) are synthesized and characterized. These ILs show low-melting point and low-viscosity characteristics, and the viscosity of OEPZ–TFSI is 41.2 mPa s at 25 °C. These IL electrolytes with 0.4 mol kg^{-1} LiTFSI have good chemical stability against lithium metal. Li/$LiFeO_4$ cells using these IL electrolytes without additives own good electrochemical performance, and the cells using OMPZ–TFSI and OEPZ–TFSI electrolytes own better rate property.

1. Introduction

During the past decade, ionic liquids (ILs) have attracted great interests of researchers due to their superior properties, including negligible volatility, nonflammability, high chemical and thermal stability, high ionic conductivity and electrochemical stability [1,2]. Due to these properties, ILs have been looked on as safe electrolytes for high energy density lithium battery, which uses lithium metal anode with high theoretical capacity of 3860 mAh g^{-1} [3,4]. Imidazolium ILs, quaternary ammonium ILs, piperidinium ILs and pyrrolidinium ILs have been investigated intensively as new electrolytes for lithium battery [5–8].

Currently, functionalized IL is a very noticeable topic in the field of IL research. Introducing different functional groups into cations, can markedly change the physicochemical properties of ILs, and it also affords more choices for applications of ILs [6]. Compared with other functional groups, ether group can reduce the viscosities and melting points of ILs without resulting in obvious degradation of electrochemical stability of ILs, and some ILs with one ether group have been used successfully as electrolytes in lithium battery [7–9].

Pyrazolium cation has the similar C–N Heterocyclic structure with imidazolium cation except the positions of the two N atoms. However, researches involving pyrazolium ILs are quite rare by contrast with imidazolium ILs. Some pyrazolium ILs without ether group have been investigated as electrolytes [10–13], catalysts for organic synthesis [14] and antibacterial cationic surfactants [15]. Recently, our group have reported two ether-functionalized pyrazolium ILs with four substituent groups in the cyclic structure of cation (1-(2-methoxyethyl)-2,3,5-Trimethylpyrazolium TFSI (2o1MPZ–TFSI) and 1-(2-methoxyethyl)-2-ethyl-3,5-Dimethylpyrazolium TFSI (2o1EPZ–TFSI)) as new electrolytes for lithium battery [16]. Though the two ILs show low melting point, their viscosities are nonideal. Decreasing the number of substituent group in the cyclic structure of cation might reduce the viscosity, such as imidazolium ILs [5,17]. In order to find low-viscosity ILs, in this work we continued to synthesize four new ether-functionalized ILs with two or three substituent

* Corresponding authors. Tel.: +86 21 54748917; fax: +86 21 54741297.
E-mail addresses: housefang@sjtu.edu.cn (S. Fang), liyangce@sjtu.edu.cn (L. Yang).

0378-7753/$ – see front matter © 2012 Elsevier B.V. All rights reserved.
http://dx.doi.org/10.1016/j.jpowsour.2012.05.082

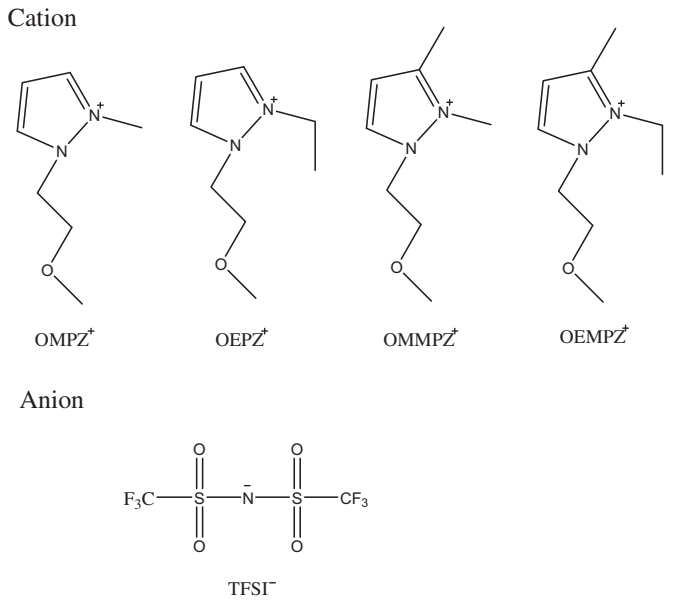

Fig. 1. Structures of cations and anion of the four functionalized ILs.

groups in the cyclic structure of pyrazolium cation, and the structures of these ILs were shown in Fig. 1. We investigated their physicochemical and electrochemical properties, and found that the four new ILs had lower viscosity than the two ether-functionalized ILs with four substituent groups in the cyclic structure of pyrazolium cation [16]. These IL electrolytes with 0.4 mol kg^{-1} LiTFSI showed good chemical stability against lithium metal. Li/$LiFeO_4$ cells using these IL electrolytes without additives owned good capacity and cycle property at the current rate of 0.1 C, and the cells using OMPZ–TFSI and OEPZ–TFSI electrolytes owned better rate property.

2. Experimental

2.1. Reagents and materials

Commercially available reagents were purchased from Sinopharm Chemical Reagent Corporation Ltd., or Alfa Aesar, and used as received. Lithium bis(trifluoromethylsulfonyl) imide (LiTFSI) was kindly provided by Morita Chemical Industries Corporation Ltd, and these reagents were all analytical grade.

2.2. Synthesis and characterization of the ILs

2.2.1. 1-(2-Methoxyethyl) pyrazole (OPZ)

Pyrazole (0.15 mol), finely ground potassium hydroxide (0.3 mol) and TBAB (Tetrabutylammonium bromide, 0.0075 mol) were sonicated with an ultrasound bath for 15 min in a 250 ml flask [18]. The 1-Bromo-2-methoxyethane (0.15 mol) was added at once in an ice bath and the reaction was stirred at the temperature for 24 h, then the product was washed with diethyl ether. The filtrate was distilled in a rotary evaporator at 60 °C and then distilled under reduced pressure using a 25 cm vigreux column. The product was collected at 49 °C–50 °C (boiling point) when the pressure was about 3 Pa. Colorless liquid; ^{1}H NMR: δ (ppm) 7.502–7.498 (d, 1H), 7.453–7.447 (d, 1H), 6.231–6.222 (t, 1H), 4.294–4.268 (t, 2H), 3.737–3.710 (t, 2H), 3.302 (s, 3H).

2.2.2. 1-(2-Methoxyethyl)-3-methylpyrazole (OM_3PZ)

3-methylpyrazole (0.15 mol), finely ground potassium hydroxide (0.3 mol) and TBAB (0.0075 mol) were sonicated with an ultrasound bath for 15 min in a 250 ml flask. The other procedures were identical with OPZ. At last, the product was collected at 58 °C–59 °C (boiling point) when the pressure was about 3 Pa. Colorless liquid; ^{1}H NMR: δ (ppm) 7.398–7.332 (d, 1H), 7.339–7.332 (d, 1H), 6.003–5.981 (q, 1H), 4.218–4.178 (q, 2H), 3.745–3.694 (m, 2H), 3.316–3.289 (d, 3H), 2.294–2.270 (d, 3H).

2.2.3. 1-(2-Methoxyethyl)-2-methylpyrazolium bis(trifluoromethanesulfonyl) imide (OMPZ–TFSI)

OPZ (7 g, 55.5 mmol) and iodomethane (8.7 g, 61.1 mmol) were dissolved in acetonitrile (10 ml) in a 250 ml flask, and the reaction lasted for 48 h in a sealed conduction at room temperature. The produced iodide was washed with Diethyl ether (3 × 30 ml), and then dried under high vacuum at 60 °C. The iodide and LiTFSI were dissolved in deionized water and mixed for 24 h at ambient temperature. The crude IL was dissolved with dichloromethane, and washed with deionized water until no residual halide anions in the deionized water used to rinse the IL could be detected by $AgNO_3$. The dichloromethane was removed by rotating evaporation and then the product was dried under high vacuum for more than 24 h at 110 °C. Colorless liquid; ^{1}H NMR: δ (ppm) 8.122–8.115 (d, 1H), 8.027–8.020 (d, 1H), 6.708–6.693 (t, 1H), 4.644–4.620 (t, 2H), 4.179 (s, 3H), 3.776–3.753 (t, 2H), 3.332 (s, 3H); ^{13}C NMR: δ (ppm) 138.253, 138.123, 137.598, 124.657–115.090, 107.865, 107.635, 77.761, 77.443, 77.122, 69.823, 69.590, 59.916, 58.559, 50.181, 49.924, 37.475, 37.181.

2.2.4. 1-(2-Methoxyethyl)-2-ethylpyrazolium bis(trifluoromethanesulfonyl) imide (OEPZ–TFSI)

OPZ (7 g, 55.5 mmol) and iodoethane (9.5 g, 61.1 mmol) were dissolved in acetonitrile (10 ml) in a 250 ml flask. The mixture was refluxed at 60 °C for 48 h under a nitrogen atmosphere. The other procedures were identical with OMPZ–TFSI. Colorless liquid; ^{1}H NMR : δ (ppm) 8.151–8.144 (d, 1H), 8.090–8.083 (d, 1H), 6.737–6.723 (t, 1H), 4.641–4.617 (t, 2H), 4.550–4.496 (q, 2H), 3.771–3.748 (t, 2H), 3.321 (s, 3H), 1.606–1.562 (t, 3H); ^{13}C NMR : δ (ppm) 137.798, 136.270, 124.675–115.102, 108.069, 77.812, 77.489, 77.168, 69.652, 58.901, 50.059, 45.941, 13.737.

2.2.5. 1-(2-Methoxyethyl)-2,3-dimethylpyrazolium bis(trifluoromethanesulfonyl) imide (OMMPZ–TFSI)

OM_3PZ (8 g, 57.1 mmol) and iodomethane (8.91 g, 62.8 mmol) were dissolved in acetonitrile (10 ml) in a 250 ml flask, the other procedures were identical with OMPZ–TFSI. Colorless liquid; ^{1}H NMR : δ (ppm) 7.976–7.968 (d, 1H), 7.915–7.908 (d, 1H), 6.495–6.467 (q, 1H), 4.568–4.521 (m, 2H), 4.093–3.966 (d, 3H), 3.734–3.650 (m, 2H), 3.310–3.282 (d, 3H), 2.474 (s, 3H); ^{13}C NMR : δ (ppm) 148.030, 147.610, 137.446, 136.490, 124.681–115.104, 108.006, 107.839, 77.781, 77.462, 77.134, 69.826, 69.524, 59.100, 58.915, 50.281, 47.405, 37.649, 33.949, 12.121.

2.2.6. 1-(2-Methoxyethyl)-2-ethyl-3-methylpyrazolium bis(trifluoromethanesulfonyl) imide (OEMPZ–TFSI)

OM_3PZ (8 g, 57.1 mmol) and iodoethane (9.8 g, 62.8 mmol) were dissolved in acetonitrile (10 ml) in a 250 ml flask. The other procedures were identical with OEPZ–TFSI. Colorless liquid; ^{1}H NMR : δ (ppm) 8.045–8.038 (d, 1H), 7.962–7.955 (d, 1H), 6.530–6.522 (d, 1H), 4.594–4.562 (m, 2H), 4.516–4.451 (m, 2H), 3.766–3.663 (m, 2H), 3.327–3.285 (d, 3H), 2.514–2.503 (d, 3H), 1.590–1.399 (m, 3H); ^{13}C NMR : δ (ppm) 148.405, 147.190, 137.098, 135.490, 124.692–115.118, 108.454, 108.240, 77.855, 77.538, 77.184, 69.603, 59.063, 58.973, 58.870, 58.797, 50.221, 47.297, 45.945, 44.592, 14.039, 13.799, 12.066, 11.778.

2.3. Measurement

^{1}H NMR and ^{13}C NMR spectra were recorded on a Bruker Avance III 400 spectrometer, and chloroform-d was used as the solvent. The

melting point was tested by using a differential scanning calorimeter (DSC, Perkin–Elmer Pyris 1) in the temperature range from −60 °C to 60 °C. An average sample weight of ca. 5 mg was sealed in an aluminum pan in a dry chamber, and then heated and cooled at a scan rate of 10 °C min^{-1}, and the thermal data was collected during heating in the second heating–cooling scan. The thermal decomposition temperature was analyzed with a thermal gravimetric analysis (Perkin Elmer, 7 series thermal analysis system). The sample with an average weight of ca. 5 mg was placed in a platinum pan and heated at 10 °C min^{-1} from ambient temperature to 600 °C under a nitrogen atmosphere. The density was affirmed by measuring the weight of prepared IL (1.0 ml) at 25 °C.

The viscosities of the two ILs and their electrolytes with 0.4 mol kg^{-1} of LiTFSI were investigated by viscometer (DV–III ULTRA, Brookfield Engineering Laboratories Inc.), and the conductivities were tested with DDS-11A conductivity meter in a dry chamber. Electrochemical window was tested by linear sweep voltammogramms (LSV) with a scan rate of 10 mV s^{-1} in an argon-filled UNLAB glove box ($[O_2] < 1$ ppm, $[H_2O] < 1$ ppm). The working electrode was glassy carbon disk (3 mm diameter), and lithium metal was used as both counter and reference electrodes. The glassy carbon electrode was polished with alumina paste ($d = 0.1$ μm), and washed with deionized water and dried under vacuum. In the LSV test, the freshly polished glassy carbon electrode was used in two scans (positive and negative, respectively) for one IL, and the fresh IL was used in each scan. The LSV test was performed by CHI660D electrochemistry workstation at room temperature (25 °C). The stability of the IL electrolyte with 0.4 mol kg^{-1} of LiTFSI against lithium was investigated by monitoring the time evolution of the impedance response for a symmetric Li/IL electrolyte/Li coin cell with the borosilicate glass separator (GF/A from Whatman), and the impedance responses were measured by using CHI660D electrochemistry workstation at room temperature (100 kHz–50 mHz; bias voltage 5 mV).

The performances of the IL electrolytes with 0.4 mol kg^{-1} of LiTFSI in lithium battery were tested with coin cells. The cathode was composed of $LiFePO_4$ (80 wt.%) as the active material, acetylene black (10 wt.%) as an electrically conductive additive, and PVDF (10 wt.%) as a binder polymer. The PVDF was dissolved in *N*-methylpyrrolidone (NMP) before used. All the materials were spreaded on aluminum current collector (battery use). Loading of active materials was about ca. 1.5–2.0 mg cm^{-2} and this thinner electrode was used without pressing. The lithium metal was used as anode, and the separator was glass filter made of borosilicate glass (GF/A, Whatman). Dried all the materials at 110 °C under vacuum and then assembled the coin cells in an argon-filled UNLAB glove box ($[O_2] < 1$ ppm, $[H_2O] < 1$ ppm). The cells were sealed and stayed for 24 h at room temperature before examined by the galvanostatic charge–discharge (C–D) cycling test using a CT2001A cell test instrument (LAND Electronic Co. Ltd.) at room temperature (25 °C), and the current rate was determined by using the nominal capacity of 170 mAh g^{-1} for Li/$LiFePO_4$ cell. Charging included two processes: (1) constant current at a rate, cut-off voltage of 4.0 V; (2) constant voltage at 4.0 V, 1 h time, and discharge had one process: constant current at the same rate, cut-off voltage of 2.0 V.

3. Result and discussion

3.1. Melting point and thermal stability

The measured data of the four ether-functionalized pyrazolium ILs, like melting point, density, viscosity, conductivity, and thermal decomposition temperature were presented in Table 1.

It had been proved that introducing one short ether group into ILs based on guanidinium cations [19–21], quaternary and cyclic quaternary ammonium cations [6,22,23], quaternary phosphonium cations [24], and imidazolium cations could be helpful to reduce the lattice energy of ILs and result in low melting point. In our previous report, replacing one alkyl group in 1,2,3,5-tetraallkylpyrazolium cations with one ether group, could also acquire the ILs with low melting point [16]. In this work, the four new ILs did not show any phase transition behaviors until −60 °C, which was the inferior temperature limit of our DSC measurement. So their melting points were also under −60 °C, and they still belonged to the ILs with low melting point.

Table 1
Physical and thermal properties of these ILs.

ILs	Mw[a]/g mol^{-1}	T_m[b]/°C	T_d[c]/°C	η[d]/mP s	σ[e]/mS cm^{-1}	d[f]/g cm^{-3}
OMPZ–TFSI	421.34	<−60	341.2	52.1	3.26	1.43
OEPZ–TFSI	435.37	<−60	338.3	41.2	3.31	1.31
OMMPZ–TFSI	435.37	<−60	356.8	73.0	2.45	1.36
OEMPZ–TFSI	449.39	<−60	344.7	68.3	2.35	1.34

[a] Molecular weight.
[b] Melting point.
[c] Decomposition temperature of 10% weight loss.
[d] Viscosity at 25 °C.
[e] Conductivity at 25 °C.
[f] Density at 25 °C.

The thermal stability of the prepared ILs was tested by TGA experiments. As shown in Fig. 2, all the four ILs had one-stage decomposition behavior, which was similar with the 1-(2-*methoxyethyl*)-2,3,5-trialkylpyrazolium ILs (2o1MPZ–TFSI and 2o1EPZ–TFSI) [16]. In terms of Table 1 and the published data [16], it could be easily found that the thermal decomposition temperature increased slightly with the increasing of the number of substituent group in the cyclic structure of pyrazolium cation. Additionally, the thermal stability of the ILs with methyl group at N-2 position was slightly better than the homologous ILs with ethyl group at N-2 position. For example, the thermal decomposition temperature increased in the following order: OEPZ–TFSI (338.3 °C) < OEMPZ–TFSI (344.7 °C) < 2o1EPZ–TFSI (355.7 °C [16]) < 2o1MPZ–TFSI (363.2 °C [16]).

3.2. Viscosities of the ILs

In our previous report, replacing one alkyl group in 1,2,3,5-tetraallkylpyrazolium cations with one ether group, could help to reduce the viscosity because the ether group was an electron-donating group which could weaken electrostatic interaction between the cation and anion [6,16]. Besides the electrostatic interaction between the cation and anion, the sizes of cation and

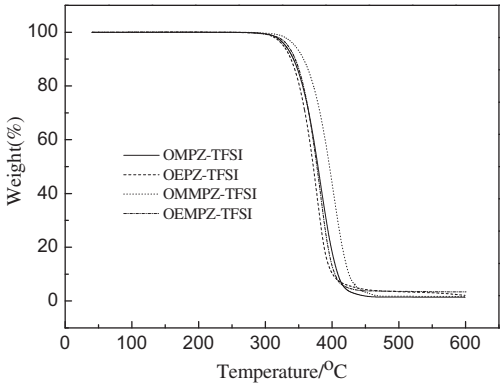

Fig. 2. TGA traces for the four ILs.

anion might also affect the viscosity of ILs. Compared the data of viscosity shown in Table 1 with 2o1MPZ–TFSI and 2o1EPZ–TFSI [16], it was apparent that the viscosities of the ILs decreased with the decreasing of the number of substituent group in the cyclic structure of pyrazolium cation, for smaller cation size would result in weaker Van der Waals interaction between cation and anion [6]. And it was interesting that the viscosity of the IL with methyl group at N-2 position was higher than the homologous IL with ethyl group at N-2 position when there were two or three substituent groups in the cyclic structure of pyrazolium cation, but the viscosity of the latter was higher when there were four substituent groups in the cyclic structure of pyrazolium cation [16]. In the four new ether-functionalized ILs, OEPZ–TFSI had lower viscosity, and the value was 41.2 mP s at 25 °C, which was also the lowest value among the pyrazolium ILs reported [10,16].

After adding lithium salts into the ILs, such as quaternary ammonium ILs [8,9], imidazolium ILs [25,26], and morpholinium ILs [26], the viscosities increased obviously. The viscosities of OMPZ–TFSI electrolyte, OEPZ–TFSI electrolyte, OMMPZ–TFSI electrolyte and OEMPZ–TFSI electrolytes with 0.4 mol kg^{-1} of LiTFSI were 100.1 mP s, 84.8 mP s, 142.0 mP s and 139.8 mP s at 25 °C.

Fig. 3 showed the temperature dependence of viscosity (η) for the four ILs and their electrolytes over the temperature range of 25–80 °C, and the Vogel–Tammann–Fulcher (VTF) plots of viscosity according to equation (1) [6] were shown in Fig. 3:

$$\eta = \eta_0 \exp\left(\frac{B}{T - T_0}\right) \quad (1)$$

where η_0 (mP s), B (K) and T_0 (K) are constants of Eq. (1). The best fit parameters of Eq. (1) were calculated and presented in Table 2. According to Fig. 3 and the values of R^2 in Table 2, the ILs and IL electrolytes were well fitted by the VTF model over the temperature range studied.

3.3. Conductivities of the ILs

The low-viscosity ILs usually displayed high ionic conductivity. In our previous paper, replacing one alkyl group in 1,2,3,5-tetraallkylpyrazolium cations with one ether group, could also improve the conductivity [16]. Like the viscosity, the sizes of cation and anion might also affect the conductivity of ILs. According to the data reported [16] and shown in Table 1, the conductivities of the ILs increased with the decreasing of the number of substituent group in the cyclic structure of pyrazolium cation. For example, the conductivities at 25 °C decreased in the following order: OMPZ–TFSI (3.260 mS cm^{-1}) > OMMPZ–TFSI (2.445 mS cm^{-1}) > 2o1MPZ–TFSI (2.228 mS cm^{-1} [16]). In the four new ether-functionalized ILs, OEPZ–TFSI had higher conductivity at 25 °C (3.309 mS cm^{-1}).

Table 2
VTF equation parameters of viscosity for these ILs.

ILs	η_0 (mPa s)	B (K)	T_0 (K)	R^2
OMPZ–TFSI	0.18 (±31.4%)	681 (±12.6%)	178 (±4.8%)	0.99971
OEPZ–TFSI	0.05 (±48.0%)	1053 (±15.9%)	141 (±9.9%)	0.9997
OMMPZ–TFSI	0.09 (±24.6%)	866 (±8.3%)	168 (±3.6%)	0.9999
OEMPZ–TFSI	0.05 (±38.2%)	1001 (±11.8%)	159 (±5.8%)	0.99982
OMPZ–TFSI electrolyte	0.18 (±11.0%)	667 (±4.0%)	192 (±1.2%)	0.99997
OEPZ–TFSI electrolyte	0.18 (±18.1%)	665 (±6.7%)	191 (±2.1%)	0.99991
OMMPZ–TFSI electrolyte	0.18 (±6.4%)	666 (±2.2%)	199 (±0.6%)	0.99999
OEMPZ–TFSI electrolyte	0.17 (±4.5%)	678 (±1.5%)	197 (±0.4%)	1

The percentage standard errors for η_0, B and T_0 had been included, and R^2 was the VTF fitting parameter.

After adding lithium salts into these pyrazolium ILs, the conductivities decreased obviously. The conductivities of OMPZ–TFSI electrolyte, OEPZ–TFSI electrolyte, OMMPZ–TFSI electrolyte and OEMPZ–TFSI electrolytes with 0.4 mol kg^{-1} of LiTFSI were 1.794 mS cm^{-1}, 2.076 mS cm^{-1}, 1.302 mS cm^{-1} and 1.228 mS cm^{-1} at 25 °C, which were still higher than 2o1MPZ–TFSI electrolyte and 2o1EPZ–TFSI electrolytes [16].

The temperature dependence of conductivity was shown in Fig. 4. The measured temperature range was from 25 °C to 80 °C, and the VTF plots of conductivity for them according to Eq. (2) were shown in Fig. 4:

$$\sigma = \sigma_0 \exp\left(\frac{B}{T - T_0}\right) \quad (2)$$

where σ_0 (mS cm^{-1}), B (K) and T_0 (K) are constants of Eq. (2). Three values and the VTF fitting parameter (R^2) for them were calculated and listed in Table 3. The temperature dependence of conductivity was also very well fitted by the VTF model over the temperature range studied.

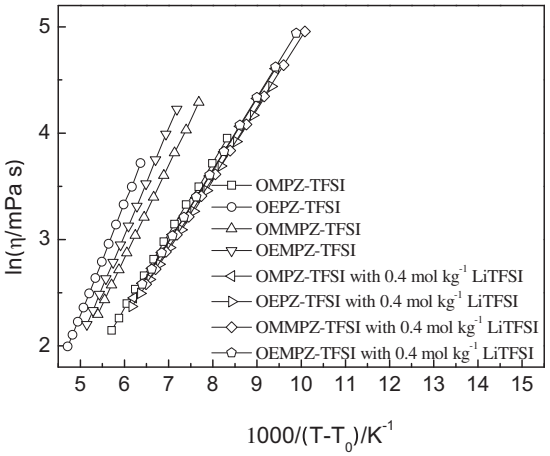

Fig. 3. VTF plots of viscosity for the four ILs and their electrolytes.

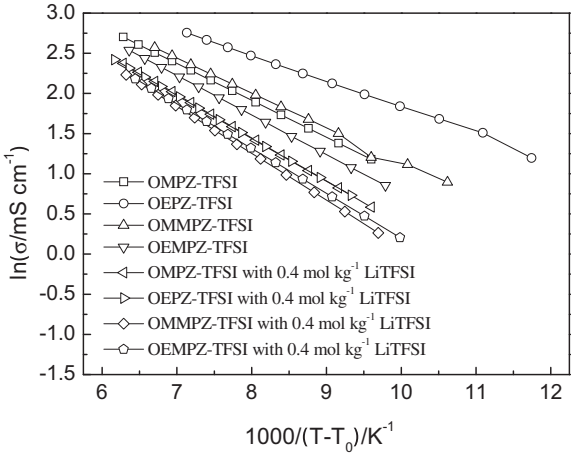

Fig. 4. VTF plots of conductivity for the four ILs and their electrolytes.

Table 3
VTF equation parameters of conductivity for these ILs.

ILs	σ_0 (mS cm^{-1})	B (K)	T_0 (K)	R^2
OMPZ–TFSI	266 (±1.4%)	458 (±0.8%)	194 (±0.3%)	1
OEPZ–TFSI	158 (±18.0%)	324 (±12.8%)	213 (±3.4%)	0.99999
OMMPZ–TFSI	249 (±31.8%)	439 (±18.1%)	204 (±5.5%)	0.99906
OEMPZ–TFSI	286 (±2.1%)	489 (±1.2%)	196 (±0.4%)	1
OMPZ–TFSI electrolyte	324 (±2.5%)	543 (±1.3%)	194 (±0.4%)	1
OEPZ–TFSI electrolyte	307 (±1.9%)	537 (±1.0%)	191 (±0.3%)	1
OMMPZ–TFSI electrolyte	367 (±3.4%)	579 (±1.6%)	195 (±0.5%)	0.99999
OEMPZ–TFSI electrolyte	327 (±2.4%)	561 (±1.1%)	198 (±0.4%)	1

The percentage standard errors for σ_0, B and T_0 had been included, and R^2 was the VTF fitting parameter.

3.4. Electrochemical windows of these ILs

The electrochemical windows were measured by linear sweep voltammogramms (LSV) using lithium metal as reference electrode. As shown in Fig. 5, OMPZ–TFSI was electrochemically stable in the range from +1.0 to +5.5 V vs. Li/Li$^+$, which indicated that its value of electrochemical window was 4.5 V at 25 °C. All the results of LSV measurements for the four functionalized ILs were listed in Table 4, which showed that the electrochemical window had no specific relationship with the number of substituent group in the cyclic structure of pyrazolium cation. The electrochemical window of OEMPZ–TFSI (4.3 V) was lower in the four ILs, and OMPZ–TFSI had higher electrochemical window. The electrochemical windows of the four ILs were higher than 4.2 V, which were better than some kinds of ILs, such as imidazolium, sulfonium and guanidinium ILs [19–21,27,28].

3.5. Chemical stabilities of the two IL electrolytes against lithium metal

The chemical stabilities of the four IL electrolytes with 0.4 mol kg^{-1} of LiTFSI against lithium metal and the interfacial characteristics of IL electrolytes/lithium metal were investigated by electrochemical impedance spectra for symmetric Li/IL electrolyte/Li cells. Fig. 6a and b showed the time evolution of the impedance response of a symmetrical Li/OEPZ–TFSI electrolyte/Li cell. The impedance responses consisted of the electrolyte bulk resistance (R_{bulk}) and the interfacial resistance (R_i), and R_{bulk} was assigned the intercept with real axis of the response at high frequency and R_i was associated the diameter of the semicircle. As shown in Fig. 6, the R_{bulk} of cell with OEPZ–TFSI electrolyte was almost unchangeable during eight days which was about 13 Ω, but its R_i fluctuated at the first 12 h, and its R_i retained about 500 Ω after some time.

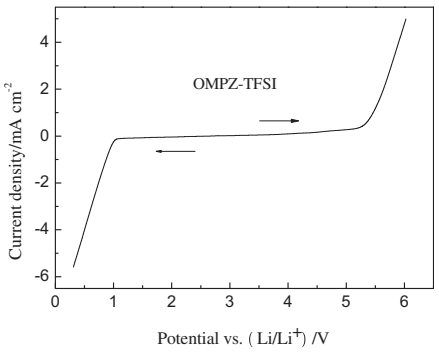

Fig. 5. Linear sweep voltammogramms of OMPZ–TFSI at 25 °C. Working electrode: glassy carbon, counter electrode: Li, reference electrode: Li, and scan rate: 10 mV s^{-1}.

Table 4
Electrochemical windows of these functionalized pyrazolium ILs.

ILs	Cathodic limiting potential	Anodic limiting potential	Electrochemical window
	V vs. Li/Li$^+$	V vs. Li/Li$^+$	V
OMPZ–TFSI	+1.0	+5.5	4.5
OEPZ–TFSI	+1.0	+5.4	4.4
OMMPZ–TFSI	+0.9	+5.3	4.4
OEMPZ–TFSI	+1.0	+5.3	4.3

Working electrode: glassy carbon; counter electrode: lithium metal; reference electrode: lithium metal; scan rate: 10 mV s^{-1}; cut-off current density: 0.1 mA cm^{-2}.

Fig. 7a and b showed the time dependence of the interfacial resistance (R_i) of the Li/IL electrolytes/Li cells. The R_i of the OMPZ–TFSI electrolyte fluctuated more obviously from 0 h to 12 h. After 24 h, the R_i of the four electrolytes became relative stable, and the stable R_i decreased in the following order: OMPZ–TFSI > OMMPZ–TFSI ≈ OEMPZ–TFSI > OEPZ–TFSI. In terms of the cathodic limiting potentials of these functionalized ILs, their IL electrolytes should react with lithium metal, and the impedance of the cells fluctuated seriously at the first 12 h, which might indicated the reaction between the electrolytes and lithium metal. The impedance became relatively stable after some time, and the experimental phenomena might indicate a passivation layer forming on the lithium metal, which could restrict the reaction between the electrolyte and lithium metal.

3.6. Battery electrolyte properties of ILs

Fig. 8 showed the performances of Li/LiFePO$_4$ cells using the four electrolytes without additive at room temperature, and the cells

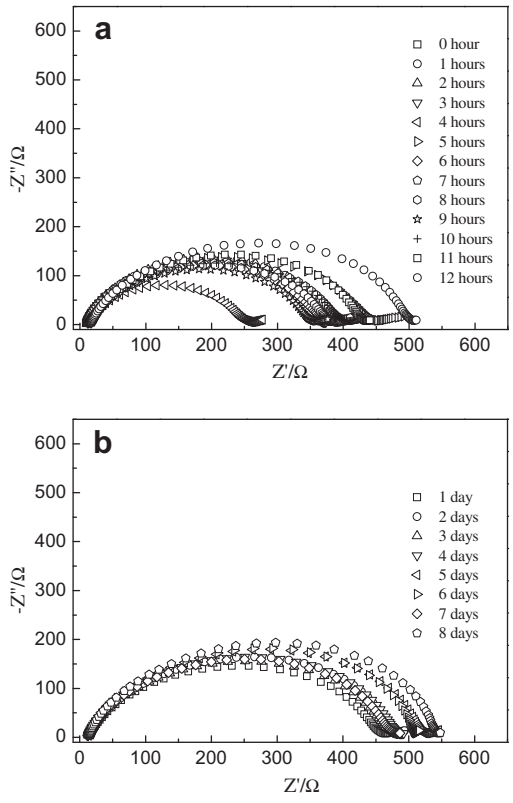

Fig. 6. Time evolution of the impedance response of a symmetrical Li/0.4 mol kg^{-1} LiTFSI in OEPZ–TFSI/Li cell: (a) from 0 h to 12 h, and (b) from 1 day to 8 days.

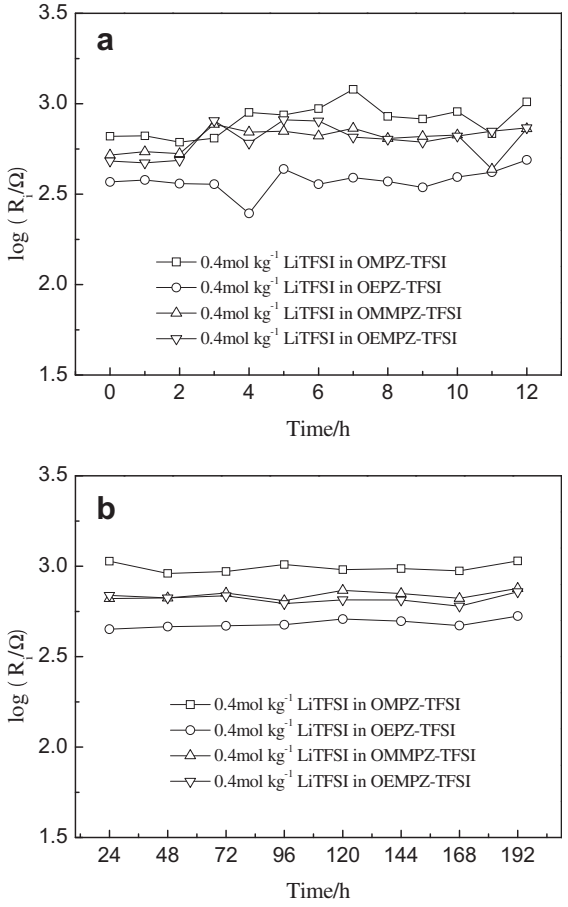

Fig. 7. Time dependence of interfacial resistance of the Li/IL electrolytes/Li cells: (a) from 0 h to 12 h, and (b) from 24 h to 192 h.

were tested under the current density of 0.1 C. The initial discharge capacity of the cells with OEPZ—TFSI electrolyte was about 132.2 mAh g^{-1}, then the discharge capacity increased with the cycle number in the following 30 cycles and stabilized at about 152 mAh g^{-1} until the 50th cycle. For the other three electrolytes, they had similar changing rule of the discharge capacity with the cycle number, and the discharge capacities stabilized at about 150 mAh g^{-1}. The discharge capacities for the four electrolytes were lower than the theoretical capacity of $LiFePO_4$ (170 mAh g^{-1})

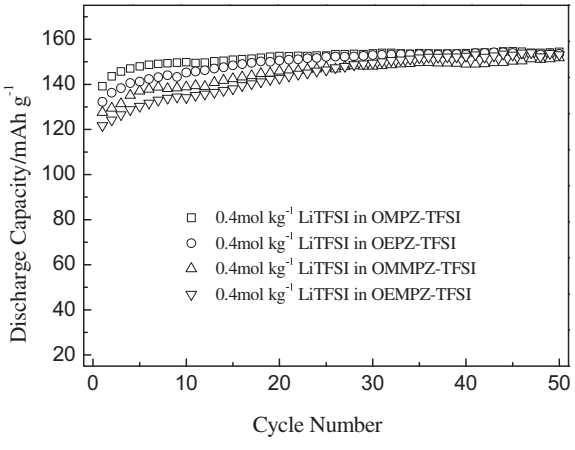

Fig. 8. Discharge capacity during cycling of Li/$LiFePO_4$ cells using the IL electrolytes. Charge—discharge current rate was 0.1 C.

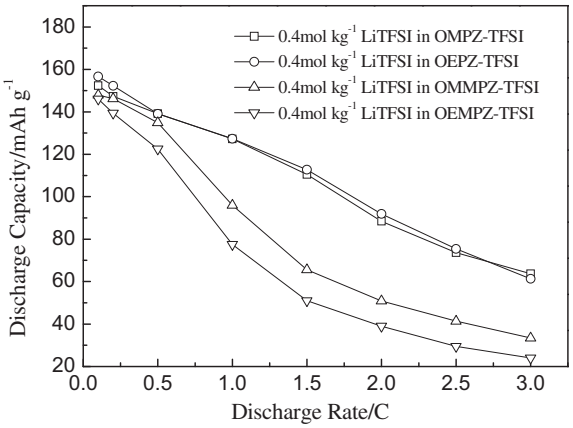

Fig. 9. Discharge capacities of Li/$LiFePO_4$ cells using the IL electrolytes at different discharge rates. Charge current rate was 0.1 C.

probably owning to the high resistance of SEI film generating on the electrode/electrolyte interface [6].

The relationships between the discharge capacities and the different discharge rates for the four IL electrolytes were shown in Fig. 9, and the discharge capacities at 0.1 C rate were the values after the cycle performances of cells reach stability. It could be found that the discharge capacity decreased with the increasing of the discharge rate for these IL electrolytes. The discharge capacity for the OEPZ—TFSI electrolyte at the discharge rate of 1.0 C was about 127.3 mAh g^{-1}, which retained 81.3% of the capacity at the rate of 0.1 C, and the discharge capacity at the rate of 2.0 C was about 91.9 mAh g^{-1}, which retained 58.7% of the capacity at the rate of 0.1 C. The rate properties of the OMPZ—TFSI and OEPZ—TFSI electrolytes were better than the OMMPZ—TFSI and OEMPZ—TFSI electrolytes, and also better than 2o1MPZ—TFSI and 2o1EPZ—TFSI electrolytes in our previous report [16]. It was obvious that the lower viscosities of OEPZ—TFSI and OMPZ—TFSI could be helpful to the rate property, because of better transport capability of lithium ion in IL electrolyte. Certainly, it was possible that the rate property was also affected by some other factors besides the viscosity of IL, such as the interfacial characteristics at both the $LiFePO_4$ cathode/electrolyte and lithium metal anode/electrolyte interfaces. Therefore, the rate property of the OMPZ—TFSI electrolyte was close to the OEPZ—TFSI electrolyte, though the viscosity of OMPZ—TFSI was higher than OEPZ—TFSI.

4. Conclusions

Four new ILs based on pyrazolium cations with one ether group and $TFSI^-$ anions were synthesized and characterized, and these ILs showed low-melting point and low-viscosity characteristics. These IL electrolytes showed good chemical stability against lithium metal owing to the formation of passivation layers. Li/$LiFePO_4$ cells using the four IL electrolytes without additives showed good electrochemical performance, and the OMPZ—TFSI and OEPZ—TFSI electrolytes had better rate properties.

Acknowledgments

The authors thank the Research Center of Analysis and Measurement of Shanghai JiaoTong University for the help in NMR characterization. This work was financially supports by the National Natural Science Foundation of China (Grants No. 21103108 and 21173148), and Key Lab of Novel Thin Film Solar Cells (Grant No. KF201110, Chinese Academy of Sciences).

References

[1] J. Dupont, R.F. De Souza, P.A.Z. Suarez, Chem. Rev. 102 (2002) 3667–3692.
[2] M. Galiński, A. Lewandowski, I. Stępniak, Electrochim. Acta 51 (2006) 5567–5580.
[3] J.R. Owen, Chem. Soc. Rev. 26 (1997) 259–267.
[4] H. Matsumoto, H. Sakaebe, K. Tatsumi, M. Kikuta, E. Ishiko, M. Kono, J. Power Sources 160 (2006) 1308–1313.
[5] C. Yan, L. Zaijun, Z. Hailang, F. Yinjun, F. Xu, L. Junkang, Electrochim. Acta 55 (2010) 4728–4733.
[6] S. Fang, Z. Zhang, Y. Jin, L. Yang, S.-i. Hirano, K. Tachibana, S. Katayama, J. Power Sources 196 (2011) 5637–5644.
[7] S. Ferrari, E. Quartarone, P. Mustarelli, A. Magistris, M. Fagnoni, S. Protti, C. Gerbaldi, A. Spinella, J. Power Sources 195 (2010) 559–566.
[8] S. Seki, Y. Ohno, H. Miyashiro, Y. Kobayashi, A. Usami, Y. Mita, N. Terada, K. Hayamizu, S. Tsuzuki, M. Watanabe, J. Electrochem. Soc. 155 (2008) A421–A427.
[9] S. Fang, Y. Tang, X. Tai, L. Yang, K. Tachibana, K. Kamijima, J. Power Sources 196 (2011) 1433–1441.
[10] S. Seki, T. Kobayashi, N. Serizawa, Y. Kobayashi, K. Takei, H. Miyashiro, K. Hayamizu, S. Tsuzuki, T. Mitsugi, Y. Umebayashi, M. Watanabe, J. Power Sources 195 (2010) 6207–6211.
[11] Y. Abu-Lebdeh, A. Abouimrane, P.J. Alarco, M. Armand, J. Power Sources 154 (2006) 255–261.
[12] P.J. Alarco, Y. Abu-Lebdeh, M. Armand, Solid State Ionics 175 (2004) 717–720.
[13] J. Čaja, T.D.J. Dunstan, H.A. Dyar, H. Krall, V. Katović, Kem. Ind./Journal of Chemists and Chemical Engineers 54 (2005) 205–214.
[14] Y. Han, H.V. Huynh, G.K. Tan, Organometallics 26 (2007) 6581–6585.
[15] N.A. Negm, M.M. Said, S.M.I. Morsy, J. Surfactants Deterg. 13 (2010) 521–528.
[16] M. Chai, Y. Jin, S. Fang, L. Yang, S.-i. Hirano, K. Tachibana, Electrochim. Acta (2012) 67–74.
[17] H. Tokuda, K. Hayamizu, K. Ishii, M.A.B.H. Susan, M. Watanabe, J. Phys. Chem. B 109 (2005) 6103–6110.
[18] E. Diez-Barra, A. Sanchez-Migallon, J. Tejeda, Synth. Commun. 20 (1990) 2849–2853.
[19] S. Fang, L. Yang, J. Wang, M. Li, K. Tachibana, K. Kamijima, Electrochim. Acta 54 (2009) 4269–4273.
[20] S. Fang, L. Yang, C. Wei, C. Jiang, K. Tachibana, K. Kamijima, Electrochim. Acta 54 (2009) 1752–1756.
[21] Y. Jin, S. Fang, L. Yang, S.-i. Hirano, K. Tachibana, J. Power Sources 196 (2011) 10658–10666.
[22] Z.B. Zhou, H. Matsumoto, K. Tatsumi, Chem. Eur. J. 11 (2005) 752–766.
[23] Z.B. Zhou, H. Matsumoto, K. Tatsumi, Chem. Eur. J. 12 (2006) 2196–2212.
[24] K. Tsunashima, M. Sugiya, Electrochem. Commun. 9 (2007) 2353–2358.
[25] M.J. Monteiro, F.F.C. Bazito, L.J.A. Siqueira, M.C.C. Ribeiro, R.M. Torresi, J. Phys. Chem. B 112 (2008) 2102–2109.
[26] M.J. Monteiro, F.F. Camilo, M.C.C. Ribeiro, R.M. Torresi, J. Phys. Chem. B 114 (2010) 12488–12494.
[27] H. Matsumoto, H. Sakaebe, K. Tatsumi, J. Power Sources 146 (2005) 45–50.
[28] S. Fang, Y. Jin, L. Yang, S.-i. Hirano, K. Tachibana, S. Katayama, Electrochim. Acta 56 (2011) 4663–4671.